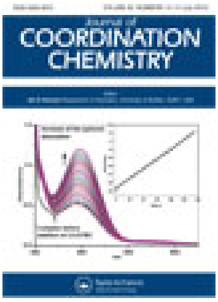

Journal of Coordination Chemistry
Publication details, including instructions for authors and subscription information:
http://www.tandfonline.com/loi/gcoo20

Intermolecular interaction and magnetic coupling mechanism between adjacent mononuclear Ni^{II} complexes

Yan-hui Chi [a], Wei Wei [b], Jing-min Shi [a], Yi-quan Zhang [c] & Shu-lian Liu [d]

[a] Key Laboratory of Molecular and Nano Probes, College of Chemistry, Chemical Engineering and Materials Science, Engineering Research Center of Pesticide and Medicine Intermediate Clean Production, Ministry of Education, Shandong Provincial Key Laboratory of Clean Production of Fine Chemicals, Shandong Normal University, Jinan 250014, P. R. China

[b] Department of Chemistry, University of California, Davis, CA 95616, USA

[c] School of Physical Science and Technology, Nanjing Normal University, Nanjing 210046, P. R. China

[d] Cadre School of Shandong Bureau of Quality and Technical Supervision, Jinan 250014, P. R. China

To cite this article: Yan-hui Chi, Wei Wei, Jing-min Shi, Yi-quan Zhang & Shu-lian Liu (2012) Intermolecular interaction and magnetic coupling mechanism between adjacent mononuclear Ni^{II} complexes, Journal of Coordination Chemistry, 65:13, 2379-2390, DOI: 10.1080/00958972.2012.694074

To link to this article: http://dx.doi.org/10.1080/00958972.2012.694074

Journal of Coordination Chemistry
Vol. 65, No. 13, 10 July 2012, 2379–2390

Taylor & Francis
Taylor & Francis Group

Intermolecular interaction and magnetic coupling mechanism between adjacent mononuclear Ni^{II} complexes

YAN-HUI CHI†, WEI WEI‡, JING-MIN SHI*†,
YI-QUAN ZHANG§ and SHU-LIAN LIU¶

†Key Laboratory of Molecular and Nano Probes, College of Chemistry, Chemical Engineering and Materials Science, Engineering Research Center of Pesticide and Medicine Intermediate Clean Production, Ministry of Education, Shandong Provincial Key Laboratory of Clean Production of Fine Chemicals,
Shandong Normal University, Jinan 250014, P. R. China
‡Department of Chemistry, University of California, Davis, CA 95616, USA
§School of Physical Science and Technology, Nanjing Normal University,
Nanjing 210046, P. R. China
¶Cadre School of Shandong Bureau of Quality and Technical Supervision,
Jinan 250014, P. R. China

(*Received 10 January 2012; in final form 3 April 2012*)

A new mononuclear complex, $[Ni(dpphen)(NCS)_2]$ [dpphen = 2,9-di(1*H*-pyrazol-1-yl)-1,10-phenanthroline], has been prepared and its crystal structure is determined by X-ray crystallography. In the Ni^{II} complex, Ni^{II} is a distorted octahedral geometry. The crystal structure analysis shows that there exist $\pi-$stacking interactions and an intermolecular interaction among adjacent complexes. The fitting to the variable-temperature magnetic susceptibility data gave the magnetic coupling constant $J = -1.37\,\mathrm{cm}^{-1}$ ($\hat{H} = -J\hat{S}_1 \cdot \hat{S}_2$). Theoretical calculations reveal that the π-stacking magnetic coupling pathway resulted in an antiferromagnetic interaction with $2J = -0.22\,\mathrm{cm}^{-1}$ ($\hat{H} = -2J\hat{S}_1 \cdot \hat{S}_2$), whereas the magnetic coupling pathway of the intermolecular interaction led to a ferromagnetic interaction with $2J = 0.10\,\mathrm{cm}^{-1}$ ($\hat{H} = -2J\hat{S}_1 \cdot \hat{S}_2$). The calculations also display that there occur both spin delocalization and spin polarization in the π-stacking magnetic coupling system and the magnetic coupling system of the intermolecular interaction.

Keywords: Crystal structure; Magnetic coupling; Intermolecular interaction; Nickel complex; Theoretical calculation; Broken-symmetry theory

1. Introduction

Molecular magnetism has attracted considerable attention, and major advances have been made in both description and applications as new molecular-based materials [1, 2]. In the area of magneto-structure correlations it is very important to obtain basic information, such as magnetic coupling signs, strength, and mechanism. In order to obtain this information, many fitting models and fitting formulas have been developed.

---

*Corresponding author. Email: shijingmin1955@gmail.com

Journal of Coordination Chemistry
ISSN 0095-8972 print/ISSN 1029-0389 online © 2012 Taylor & Francis
http://dx.doi.org/10.1080/00958972.2012.694074

Theoretical calculations have also been successfully developed and practiced on binuclear and trinuclear models in order to reveal the factors that dominate magnetic coupling properties. Mostly, fittings and calculations deal with systems with coupling spin-carriers (or paramagnetic centers) linked by bridging ligands, namely, the magnetic interactions are through bond exchange [3–7]. In magnetic coupling, intermolecular interaction also plays an important role. For example, some authors attribute the strong ferromagnetic order to the π–π stacking interaction [8] and other authors found that the π–π stacking interaction led to a strong anti-ferromagnetic interaction between spin-carriers [9–11]; strong anti-ferromagnetic coupling between Cu^{II} ions through O–H $\cdots$ O hydrogen bonding has also been reported [12]. Intermolecular force should be a key factor that dominates magnetic coupling properties. However, not much work is published on the π–π stacking [8–11], hydrogen bonds [13–20] and X–H $\cdots\pi$ interaction systems [16]. Most of these papers only deal with radicals [13, 20] or complexes [11, 21–24] with radicals as ligands. Factors that dominate magnetic coupling properties have not been clearly understood. Thus, it is important to design and synthesize complexes with intermolecular interactions and to study the factors that dominate magnetic coupling mechanism, an area to which our attention has been given [25–30].

2,9-Di(1*H*-pyrazol-1-yl)-1,10-phenanthroline is an ideal ligand possessing strong chelated coordination and larger conjugation planes, which may be useful to form complexes with both strong π-stacking and relevant magnetic coupling pathway. Some of these intermolecular forces could be effective magnetic coupling pathways leading to interesting magnetic interactions. Herein, we report a Ni^{II} complex with 2,9-di(1*H*-pyrazol-1-yl)-1,10-phenanthroline as ligand and its magnetic coupling mechanism arising from intermolecular forces, studied experimentally and by theoretical calculations.

2. Experimental

2.1. *Materials*

2,9-Di(1*H*-pyrazol-1-yl)-1,10-phenanthroline was synthesized by the reaction of 2,9-dichloro-1,10-phenanthroline and pyrazole as follows. Pyrazole (1.020 g, 1.5×10^{-2} mol), potassium carbonate (4.14 g, 3×10^{-2} mol), and tetrabutyl ammonium bromide (0.215 g, 6.67×10^{-4} mol) were added into a tetrahydrofuran solution (90 mL) containing 2,9-dichloro-1,10-phenanthroline (1.245 g, 5×10^{-3} mol) and the solution was refluxed for 72 h. After the solvent was removed by distillation under reduced pressure, ice water (60 mL) was added and the mixture was stirred for 10 h. The yellowish sediment was collected by filtration and washed with distilled water until the eluent was neutral; drying gave 1.08 g of pure 2,9-di(1*H*-pyrazol-1-yl)-1,10-phenanthroline. All other chemicals were of analytical grade and used without purification.

2.2. *Preparation of complex*

Methanol solution (5 mL) of $Ni(ClO_4)_2{\cdot}6H_2O$ (0.0713 g, 1.95×10^{-4} mol) was added into 15 mL dichloromethane solution of 2,9-di(1*H*-pyrazol-1-yl)-1,10-phenanthroline

(0.0304 g, 9.74×10^{-5} mol), and then 5 mL methanol solution of NaSCN (0.01579 g, 1.95×10^{-4} mol) was added. The mixed solution was stirred for a few minutes. Green single crystals appeared after the filtrate was allowed to slowly evaporate at room temperature for 6 days. The sample was obtained by filtration. IR (cm^{-1}): 2103(s), 1597(s), 1534(m), 1486(m), 1396(s), 1154(m), 1035(s). Elemental Anal. Calcd for $C_{20}H_{12}N_8NiS_2$ (%): (Fw 487.21) C, 49.30; H, 2.49; N, 23.00; Ni, 12.05. Found (%): C, 49.58; H, 2.71; N, 22.67; Ni, 12.61.

2.3. *Physical measurements*

Infrared spectra were recorded with a Bruker Tensor 27 infrared spectrometer from 4000 to 500 cm^{-1} using KBr disks. C, H, and N elemental analyses were carried out on a Perkin Elmer 240 instrument and nickel analysis was performed on an atomic absorption spectrophotometer, Model Z-8000. UV-Vis solid reflectance spectrum was recorded on a spectrophotometer UV-Lambda 35. Variable-temperature magnetic susceptibilities of microcrystalline powder samples were measured in a magnetic field of 1 kOe from 2.00 to 300 K on a SQUID magnetometer and the data were corrected for magnetization of the sample holder and for the diamagnetic contributions of the complex which were estimated from Pascal's constants.

2.4. *Computational details*

The magnetic interactions between metal ions were studied by density functional theory (DFT) coupling with the broken-symmetry approach (BS) [31–33]. The exchange coupling constants J have been evaluated by the energy difference between the high-spin state (E_{HS}) and the broken-symmetry state (E_{BS}). Assuming the spin Hamiltonian is defined as:

$$\hat{H} = -2J\hat{S}_1 \cdot \hat{S}_2 \tag{1}$$

if the spin projected approach is used, the equation proposed by Noodleman [31–33] to extract the J value for a binuclear transition metal complex is thus

$$J = \frac{E_{BS} - E_{HS}}{4S_1S_2} \tag{2}$$

To obtain exchange coupling constants J, Orca 2.8.0 calculations [34] were performed with the popular spin-unrestricted hybrid functional B3LYP proposed by Beck [35, 36] and Lee *et al.* [37], which can provide J values in agreement with the experimental data for transition metal complexes [38, 39]. Tri-ζTri-z with one polarization function def2-TZVP [40, 41] basis set proposed by Ahlrichs and co-workers for all atoms was used in our calculations. Strong convergence criteria were used in order to ensure that the results are well converged with respect to technical parameters (the system energy was set to be smaller than 10^{-7} hartree).

2.5. *X-ray crystallographic analysis of the complexes*

A single crystal of the complex with dimensions $0.50 \times 0.35 \times 0.16$ mm^3 was chosen under an optical microscope and subsequently glued to the tip of a glass fiber.

Table 1. Crystal data and structure refinements for the complex.

Empirical formula	$C_{20}H_{12}N_8NiS_2$
Formula weight	487.21
Temperature (K)	298(2)
Crystal system	Monoclinic
Space group	$C2/c$
Unit cell dimensions (Å, °)	
a	12.734(2)
b	17.272(3)
c	9.2099(16)
α	90.00
β	93.596(2)
γ	90.00
Volume (Å^3), Z	2021.6(6), 4
Calculated density ($g \cdot cm^{-1}$)	1.601
Absorption coefficient (mm^{-1})	1.193
Reflections collected	5032
Independent reflection	1782 [R(int) = 0.0269]
Final R indices [$I > 2\sigma(I)$]	$R_1 = 0.0311$, $wR_2 = 0.0889$
Goodness-of-fit on F^2	1.056
Largest difference peak and hole (e Å^{-3})	0.358 and −0.215

Table 2. Selected bond lengths (Å) and angles (°) for the complex.

Ni1–N1	2.3570(19)	Ni1–N4	1.9811(18)	Ni1–N2	2.0430(17)
N1–Ni1–N2	71.66(7)	N1–Ni1–N4	87.23(7)	N1–Ni1–N1	138.45(7)
N1–Ni1–N2	149.89(7)	N1–Ni1–N4	87.36(7)	N2–Ni1–N4	95.46(7)
N2–Ni1–N1	149.89(7)	N2–Ni1–N2	78.24(7)	N2–Ni1–N4	96.42(7)
N4–Ni1–N1	87.36(7)	N4–Ni1–N2	96.42(7)	N4–Ni1–N4	164.68(8)

The determination of crystal structure at 25°C was carried out on an X-ray diffractometer (Bruker Smart-1000 CCD) using graphite monochromated Mo-Kα radiation ($\lambda = 0.71073$ Å). Corrections for L_p factors were applied and all non-hydrogen atoms were refined with anisotropic thermal parameters. The hydrogen atoms were placed in calculated positions and refined as riding. The programs for the structure solution and refinement were SHELXS-97 and SHELXL-97, respectively [42]. The pertinent crystallographic data collection and structural refinement parameters for the complex summarized in tables 1 and 2 show the coordination bond lengths and the associated angles.

3. Results and discussion

3.1. *Structure description*

Figure 1 shows the coordination and atom numbering scheme. The data in table 2 display that the coordination bond lengths are 1.9811(18) Å to 2.3570(19) Å and the associated angles change from 71.66(7)° to 164.68(8)°. Ni1 assumes a distorted octahedral geometry. The non-hydrogen atoms of 2,9-di(1*H*-pyrazol-1-yl)-1,10-phenanthroline define a plane within 0.0360 Å with a maximum deviation of

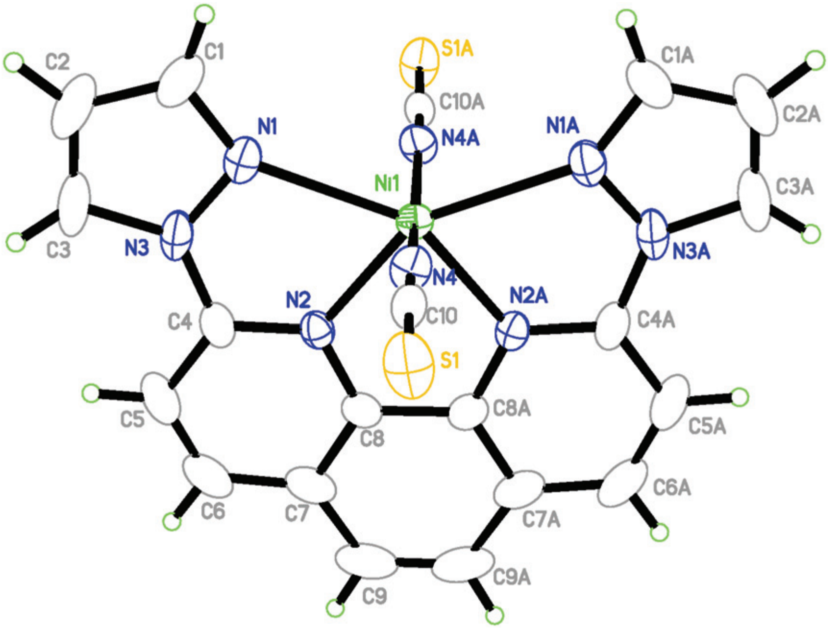

Figure 1. Coordination diagram of the complex with the atom numbering scheme (symmetry code:A = $-x+1$, y, $-z+5/2$).

−0.0572(20) Å for C6. In the crystal, there is a slipped $\pi-\pi$ stacking [43] among adjacent complexes with name PS-1, as shown in figure 2, which involves 1,10-phenanthrolin-2,9-bispyrazolyl ring and its symmetry-related counterpart, with an interplanar distance of 3.547 Å. In the PS-1 system, there are four pairs of non-bonded atoms with separation distances less than the sum of the default contact radii [44], namely, H5 ··· C20A, 2.674(3) Å; H5 ··· S2A, 2.982(1) Å; H5A ··· C20, 2.674(3) Å; H5A ··· S2, 2.982(1) Å; and another four pairs of non-bonded atoms with a separation distance less than 3.6 Å [N3 ··· C5A, 3.463(4) Å; N3A ··· C5, 3.463(4) Å; C3 ··· C6A, 3.514(5) Å; C3A ··· C6, 3.514(5) Å]. In addition to the $\pi-\pi$ stacking, there also exists an intermolecular interaction (figure 3) between adjacent complexes through short contacts of relevant non-bonded atoms, namely, C11–H1 ··· C10A, 2.860(2) Å with name IM-1. The $\pi-\pi$ stacking and the short contacts may solidify the crystal.

3.2. *UV-Vis solid electronic reflectance spectrum*

Figure 4 displays the UV-Vis solid electronic reflectance spectrum and it shows two broad bands centered at 531 and 740 nm, respectively. The two d–d bands should be assigned to transitions $^3T_{1g}(P) \leftarrow {}^3A_{2g}$ (ν_3) and $^3T_{1g}(F) \leftarrow {}^3A_{2g}(\nu_2)$, respectively [45].

3.3. *Magnetic study*

3.3.1. Experimental result. The experimental data of variable-temperature (2.00–300 K) magnetic susceptibility of the complex is shown in figure 5, where χ_M is the

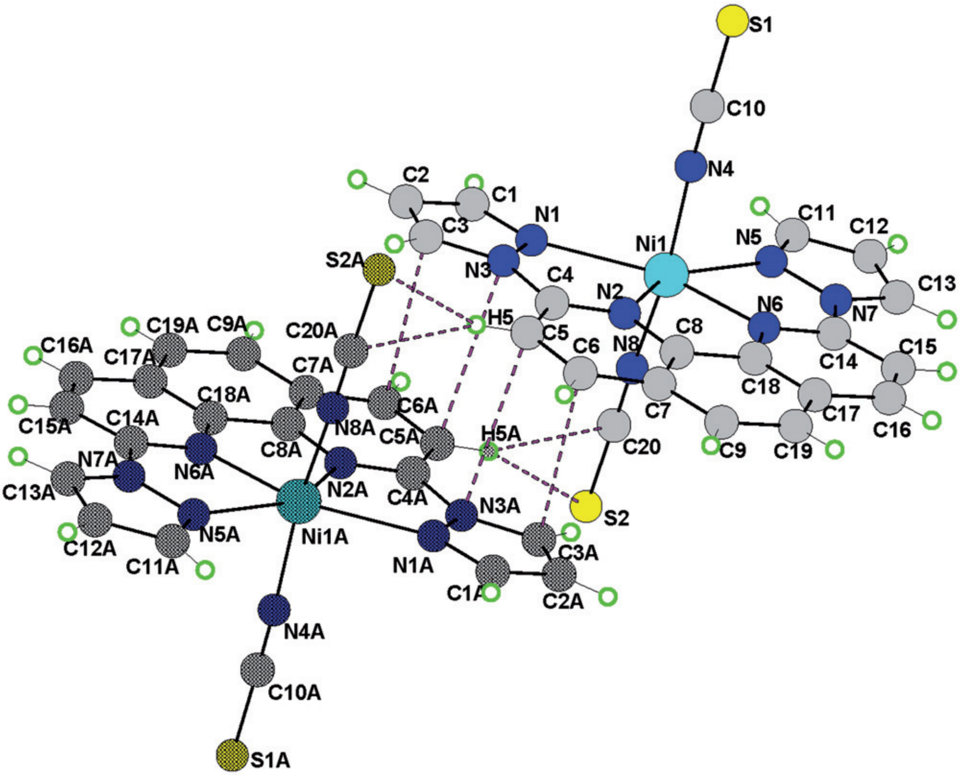

Figure 2. The π-stacking between adjacent complexes for model 1.

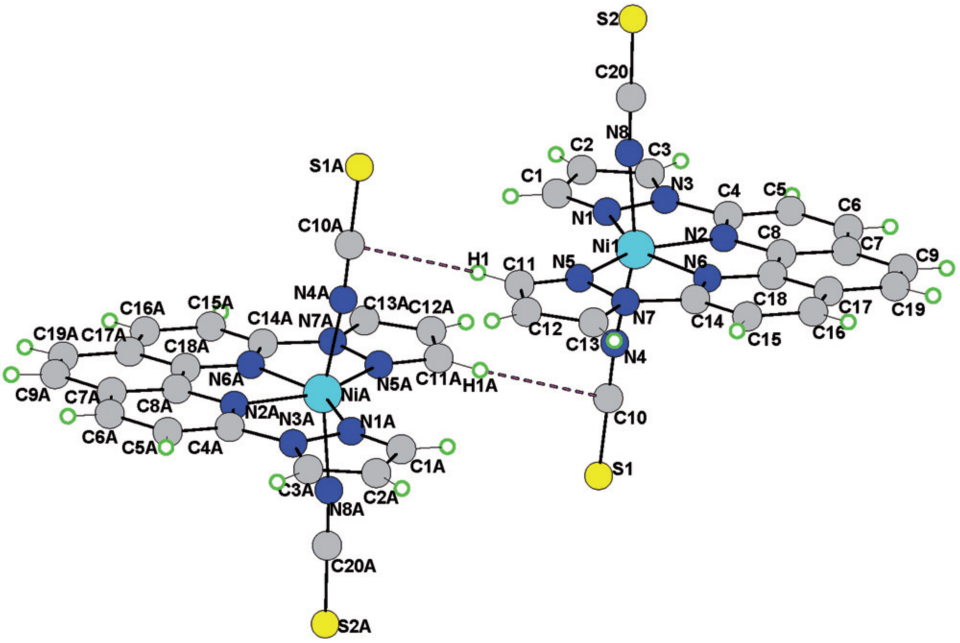

Figure 3. The intermolecular interaction between the adjacent complexes for model 2.

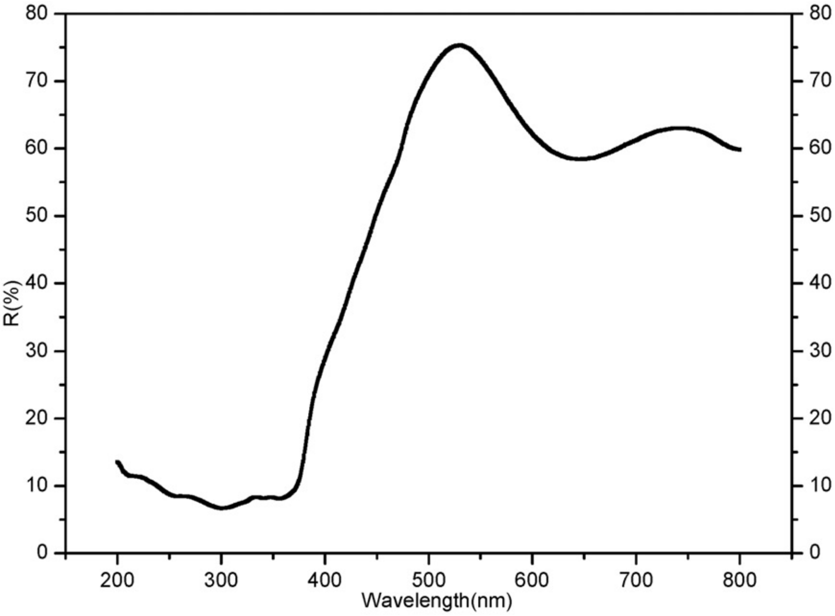

Figure 4. UV-Vis solid electronic reflectance spectrum.

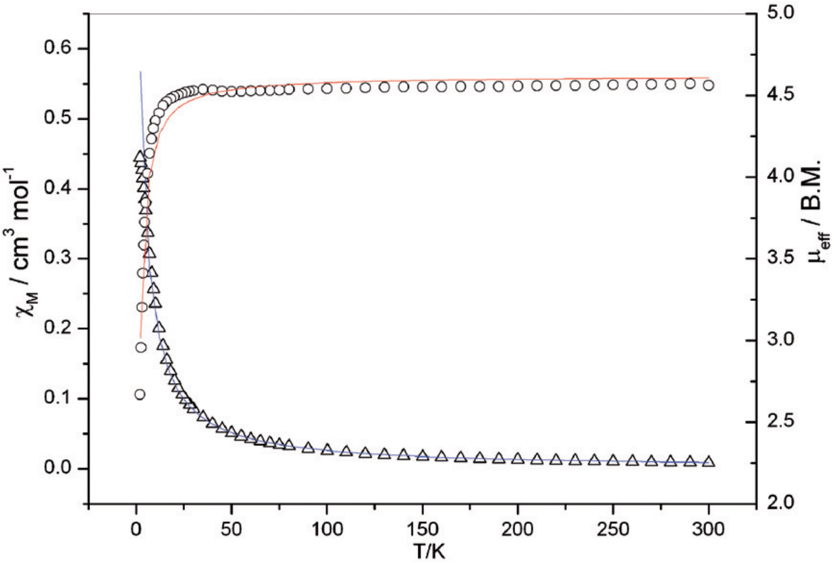

Figure 5. Plots of χ_M (the open triangle for the experimental data and the blue curve for the fitting values) and μ_{eff} (the open circle for the experimental data and the red curve for the fitting value) *vs.* T for the Ni^{II} complex.

molar magnetic susceptibility per binuclear Ni^{II} unit and μ_{eff} is the magnetic moment per binuclear Ni^{II} unit. The μ_{eff} value at 300 K is 4.56 B.M., larger than that of the isolated binuclear Ni^{II} ions (4.00 B.M., $g = 2$) at room temperature. The value of μ_{eff} decreases very slowly with the drop on temperature until 16.0 K and then starts to decrease sharply to 2.67 B.M. at 2.00 K, which indicates that there is a weak antiferromagnetic interaction between adjacent $\mathrm{Ni^{II}}$ ions. The binuclear $\mathrm{Ni^{II}}$ fitting formula (4) [46], which was obtained based on the isotropic Hamiltonian, as presented in equation (3), was used to fit the experimental susceptibility data.

$$\hat{H} = -J\hat{S}_1 \cdot \hat{S}_2 \tag{3}$$

$$\chi = \frac{2Ng^2\beta^2}{\kappa T}\frac{\exp(\frac{J}{\kappa T}) + 5\exp(\frac{3J}{\kappa T})}{1 + 3\exp(\frac{J}{\kappa T}) + 5\exp(\frac{3J}{\kappa T})} \tag{4}$$

$$\chi_M = \frac{\chi}{1 - \frac{zJ'\chi}{Ng^2\beta^2}} \tag{5}$$

Equation (5) gave a good fit to the experimental data, as shown in figure 5, and the relevant fitting parameters are: $g = 2.31$, $J = -1.37\,\mathrm{cm^{-1}}$, $zJ' = -0.10\,\mathrm{cm^{-1}}$ and $R = \Sigma(\chi_{\mathrm{obsd}} - \chi_{\mathrm{calcd}})^2/(\chi_{\mathrm{obsd}})^2 = 4.7 \times 10^{-4}$. The fitting for the data of the variable-temperature susceptibility with the Curie–Weiss formula gave the Weiss constant $\theta = -2.48\,\mathrm{K}$, as shown in figure 6. Both the values $J = -1.37\,\mathrm{cm^{-1}}$ and $\theta = -2.48\,\mathrm{K}$ indicate that there is a very weak antiferromagnetic interaction between the adjacent $\mathrm{Ni^{II}}$ ions. Because there are π–π stacking and short contacts between adjacent complexes and each intermolecular force means a possible magnetic coupling pathway, theoretical calculations were performed to understand the magnetic coupling mechanisms involved in the relevant magnetic coupling pathways.

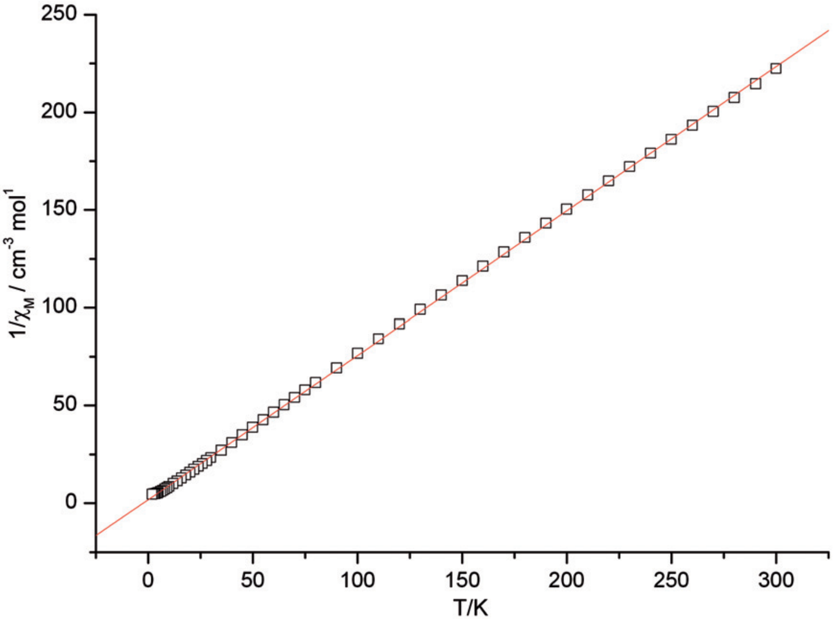

Figure 6. Thermal variation of reciprocal susceptibility (open square for experimental data and red line for the theoretical values).

3.3.2. Theoretical study on magnetic interactions. Density function calculations were based on models 1 and 2, as shown in figures 7 and 8, which stand for PS-1 and IM-1 magnetic coupling pathways, respectively. The calculations were constrained by bond lengths, associated angles, and relevant locations of adjacent complexes from the X-ray structure.

According to equation (2), calculations gave $2J$ values of $-0.22\,\text{cm}^{-1}$ (or $J = -0.11\,\text{cm}^{-1}$ with $\hat{H} = -J\hat{S}_1 \cdot \hat{S}_2$) and $0.10\,\text{cm}^{-1}$ (or $J = 0.05\,\text{cm}^{-1}$ with $\hat{H} = -J\hat{S}_1 \cdot \hat{S}_2$) for models 1 and 2, respectively, which means that PS-1 magnetic coupling pathway resulted in a very weak antiferromagnetic interaction, whereas IM-1 magnetic coupling pathway led to a very weak ferromagnetic interaction. Based on the fact that these magnetic interactions must offset each other and the antiferromagnetic coupling strength is larger than that of the ferromagnetic coupling, the overall magnetic interaction should be an antiferromagnetic interaction, which is consistent with the experimental result. In the two models, separation distances of Ni1 ··· Ni1A are 8.233(7) Å for PS-1 and 7.188(1) Å for IM-1, which implies that these magnetic interactions are not from the dipole–dipole interaction due to the stronger magnetic interaction not arising from the short separation distance of Ni1 ··· Ni1A. Theoretical calculations also gave spin density population of the ground state of the two systems. For each system, the absolute value of the spin density population of each Ni^{II} is smaller than 2 and the coordinated atoms exhibit the same sign as the relevant Ni^{II}, suggesting that spin delocalization from Ni^{II} 3d orbitals to relevant coordinated atoms occurs. At the same time, there exists spin-polarization in the two systems because some atoms exhibit different spin sign from that of relevant Ni^{II} ions. Both the spin

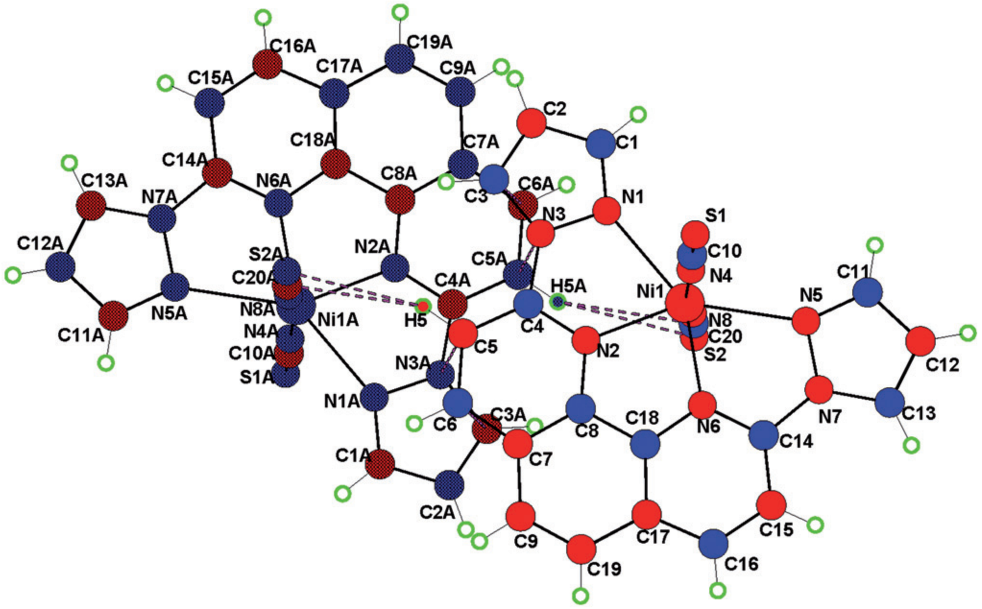

Figure 7. The calculated spin density population for model 1, in which the atoms with positive spin density are drawn in red (C2, C5, C7, C9, C12, C15, C17, C19, N1, N2, N3, N4, N5, N6, N7, N8, S1, S2, H5, Ni1, C1A, C3A, C4A, C6A, C8A, C10A, C11A, C13A, C14A, C16A, C18A, C20A) and the atoms with negative spin density in blue (C1, C3, C4, C6, C8, C10, C11, C13, C14, C16, C18, C20, C2A, C5A, C7A, C9A, C12A, C15A, C17A, C19A, N1A, N2A, N3A, N4A, N5A, N6A, N7A, N8A, S1A, S2A, H5A, Ni1A).

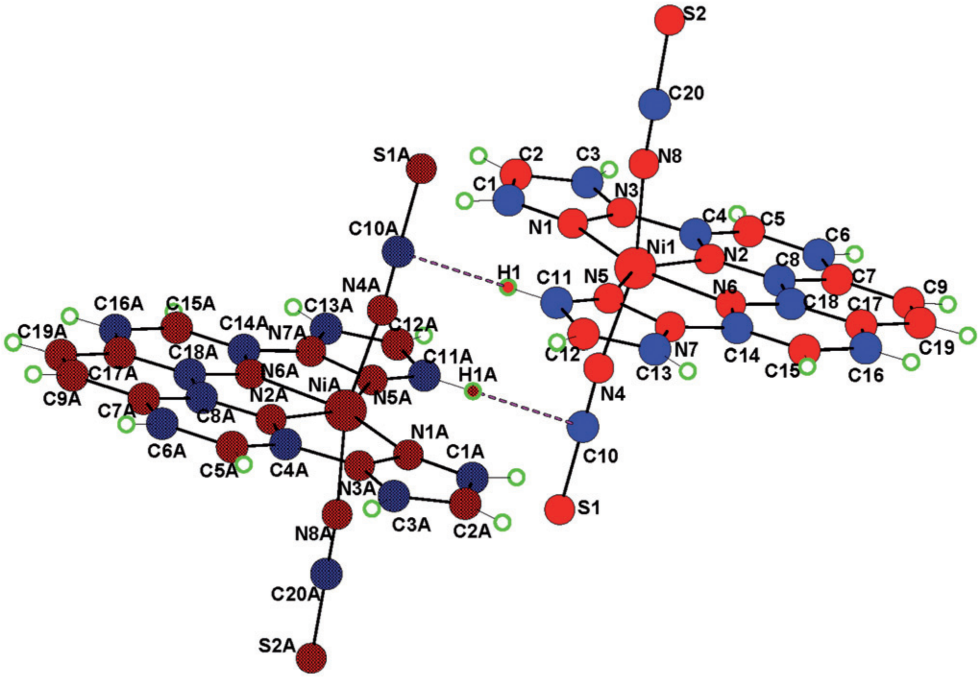

Figure 8. The calculated spin density population for model 2, in which the atoms with positive spin density are drawn in red (C2, C5, C7, C9, C12, C15, C17, C19, N1, N2, N3, N4, N5, N6, N7, N8, S1, S2, H1, Ni1, C2A, C5A, C7A, C9A, C12A, C15A, C17A, C19A, N1A, N2A, N3A, N4A, N5A, N6A, N7A, N8A, S1A, S2A, H1A, Ni1A) and atoms with negative spin density are drawn in blue (C1, C3, C4, C6, C8, C10, C11, C13, C14, C16, C18, C20, C1A, C3A, C4A, C6A, C8A, C10A, C11A, C13A, C14A, C16A, C18A, C20A).

delocalization and the spin-polarization may benefit the magnetic coupling interaction in each intermolecular magnetic coupling pathway.

4. Conclusions

A new Ni^{II} mononuclear complex with 2,9-di(1*H*-pyrazol-1-yl)-1,10-phenanthroline has been synthesized and its crystal structure are determined. It displays a π–π stacking interaction and an intermolecular force among adjacent complexes. The fitting for the data of the variable-temperature magnetic susceptibilities indicates that there exists a weak antiferromagnetic interaction with $J = -1.37\,\mathrm{cm}^{-1}$. Theoretical calculations further reveal that the weak antiferromagnetic interaction should be from the cooperation of the very weak antiferromagnetic interaction of the π–π stacking and the very weak ferromagnetic interaction of the intermolecular short contact.

Supplementary material

CCDC 782566 contains detailed information of the Crystallographic data for this article, and these data can be obtained free of charge from the Cambridge Crystallographic Data Centre *via* http://www.ccdc.cam.ac.uk/data_request/cif

Acknowledgments

This work was supported by the National Natural Science Foundation of China (Grant No. 20971080), the National Natural Science Foundation for the Youth of China (Grant No. 10704041), and the Natural Science Foundation of Shandong Province (Grant No. ZR2009BM026).

References

[1] G.L.J.A. Rickken, E. Raupack. *Nature*, **405**, 932 (2000).

[2] S. Tanase, J. Reedijk. *Coord. Chem. Rev.*, **250**, 2501 (2006).

[3] H. Li, T.-T. Sun, S.-G. Zhang, J.-M. Shi. *J. Coord. Chem.*, **63**, 1531 (2010).

[4] C. Wang, J. Li, Y.-W. Ren, F.-G. He, G. Meke, F.-X. Zhang. *J. Coord. Chem.*, **61**, 4033 (2008).

[5] H. Li, C. Hou, J.-M. Shi, S.-G. Zhang. *J. Coord. Chem.*, **61**, 3501 (2008).

[6] J.-M. Li, X. Jin. *J. Coord. Chem.*, **62**, 2610 (2009).

[7] J.-M. Shi, Q.S. Liu, W. Shi. *J. Coord. Chem.*, **62**, 1121 (2009).

[8] L.-L. Li, K.-J. Lin, C.-J. Ho, C.-P. Sun, H.-D. Yang. *Chem. Commun.*, 1286 (2006).

[9] N.P. Gritsan, A.V. Lonchakov, E. Lork, R. Mews, E.A. Pritchina, A.V. Zibarev. *Eur. J. Inorg. Chem.*, 1994 (2008).

[10] K. Goto, T. Kubo, K. Yamanoto, K. Nakasuji, K. Sato, D. Shiomi, T. Takui, M. Kubota, T. Kobayashi, K. Yakusi, J. Ouyang. *J. Am. Chem. Soc.*, **121**, 1619 (1999).

[11] B.D. Koivisto, A.S. Ichimura, R. McDonald, M.T. Lemaire, L.K. Thompson, R.G. Hicks. *J. Am. Chem. Soc.*, **128**, 690 (2006).

[12] J.A. Bertrand, T.D. Black, P.G. Eller, F.T. Helm, R. Mahmood. *Inorg. Chem.*, **15**, 2965 (1976).

[13] D. Maspoch, L. Catala, P. Gerbier, D. Ruiz-Molina, J. Vidal-Gancedo, K. Wurst, C. Rovira, J. Veciana. *Chem. Eur. J.*, **8**, 3635 (2002).

[14] J.L. Manson, J.A. Schlueter, K.A. Funk, H.I. Southerland, B. Twamley, T. Lancaster, S.J. Blundell, P.J. Baker, F.L. Pratt, J. Singleton, R.D. McDonald, P.A. Goddard, P. Sengupta, C.D. Batista, L. Ding, C. Lee, M.-H. Whangbo, I. Franke, S. Cox, C. Baines, D. Tria. *J. Am. Chem. Soc.*, **131**, 6733 (2009).

[15] J. Tang, J.S. Costa, A. Golobic, B. Kozlevcar, A. Robertazzi, A.V. Vargiu, P. Gamez, J. Reedijk. *Inorg. Chem.*, **48**, 5473 (2009).

[16] B. Sarkar, S. Konar, C.J. Gomez-Garcıa, A. Ghosh. *Inorg. Chem.*, **47**, 11611 (2008).

[17] M.S. Ray, A. Ghosh, R. Bhattacharya, G. Mukhopadhyay, M.G.B. Drew, J. Ribas. *Dalton Trans.*, **33**, 252 (2004).

[18] M.S. Ray, A. Ghosh, S. Chaudhuri, M.G.B. Drew, J. Ribas. *Eur. J. Inorg. Chem.*, 3110 (2004).

[19] W.-Z. Shen, X.-Y. Chen, P. Cheng, S.-P. Yan, B. Zhai, D.-Z. Liao, Z.-H. Jiang. *Eur. J. Inorg. Chem.*, 2297 (2005).

[20] C. Rancurel, N. Daro, O.B. Borobia, E. Herdtweck, J.-P. Sutter. *Eur. J. org. Chem.*, 167 (2003).

[21] C. Faulmann, E. Riviere, S. Dorbes, F. Senocq, E. Coronado, P. Cassoux. *Eur. J. Inorg. Chem.*, 2880 (2003).

[22] L. Norel, F. Pointillart, C. Train, L.-M. Chamoreau, K. Boubekeur, Y. Journaux, A. Brieger, D.J.R. Brook. *Inorg. Chem.*, **47**, 2396 (2008).

[23] X.M. Ren, S. Nishihara, T. Akutagawa, S. Noro, T. Nakamura. *Inorg. Chem.*, **45**, 2229 (2006).

[24] C.-B. Liu, Y.-M. Sun, B. Zheng, R.-X. Wang. *Chem. Phys. Lett.*, **411**, 416 (2005).

[25] J.M. Shi, X.Z. Meng, Y.M. Sun, H.Y. Xu, W. Shi, P. Cheng, L.D. Liu. *J. Mol. Struct.*, **917**, 164 (2009).

[26] L. Yu, J.M. Shi, Y.Q. Zhang, Y.Q. Wang, Y.N. Fan, G.Q. Zhang, W. Shi, P. Cheng. *J. Mol. Struct.*, **987**, 138 (2011).

[27] C. Hou, J.M. Shi, Y.M. Sun, W. Shi, P. Cheng, L.D. Liu. *Dalton Trans.*, **37**, 5970 (2008).

[28] Y.H. Chi, L. Yu, J.M. Shi, Y.Q. Zhang, T.Q. Hu, G.Q. Zhang, W. Shi, P. Cheng. *Dalton Trans.*, **40**, 1453 (2011).

[29] H. Li, S.-G. Zhang, L.-M. Xie, L. Yu, J.-M. Shi. *J. Coord. Chem.*, **64**, 1456 (2011).

[30] H. Li, S.-G. Zhang, L.-M. Xie, L. Yu, J.-M. Shi. *J. Coord. Chem.*, **64**, 3595 (2011).

[31] L. Noodleman. *J. Chem. Phys.*, **74**, 5737 (1981).

[32] L. Noodleman, E.J. Baerends. *J. Am. Chem. Soc.*, **106**, 2316 (1984).

[33] L. Noodleman, D.A. Case. *Adv. Inorg. Chem.*, **38**, 423 (1992).

[34] F. Neese. *An Ab Initio, DFT and Semiempirical Electronic Structure Package*, Program Version 2.7, Revision 0; Lehrstuhl fuer Theoretische Chemie Institut fuer Physikalische und Theoretische Chemie, Universitaet Bonn, Germany (2010).

[35] A.D. Beck. *J. Chem. Phys.*, **98**, 5648 (1993).
[36] A.D. Beck. *Phys. Rev. A*, **38**, 3098 (1988).
[37] C. Lee, W. Yang, R.G. Parr. *Phys. Rev. B*, **37**, 785 (1988).
[38] J. Cano, E. Ruiz, S. Alvarez, M. Verdaguer. *Comments Inorg. Chem.*, **20**, 27 (1998).
[39] E. Ruiz, P. Alemany, S. Alvarez, J. Cano. *J. Am. Chem. Soc.*, **119**, 1297 (1997).
[40] H.-Kr.A. Schaefer, H. Horn, R. Ahlrichs. *J. Chem. Phys.*, **97**, 2571 (1992).
[41] F. Weigend, R. Ahlrichs. *Phys. Chem. Chem. Phys.*, **7**, 3297 (2005).
[42] Bruker. *SHELXTL*, Bruker AXS Inc., Madison, WI, USA (2001).
[43] C. Janiak. *J. Chem. Soc., Dalton Trans.*, 3885 (2000).
[44] A. Bondi. *J. Phys. Chem.*, **68**, 441 (1964).
[45] J.M. Shi, D.Z. Liao, Z.H. Jiang, G.L. Wang. *Polish J. Chem.*, **69**, 346 (1995).
[46] P. Vitoria, I. Muga, J.M. Gutierrez-Zorrilla, A. Luque, P. Roman, L. Lezama, F.J. Zuniga, J. Beitia. *Inorg. Chem.*, **42**, 960 (2003).